Magnetization of planar four-fermion systems

Heron Caldas[1,*] and Rudnei O. Ramos[2,†]
[1]*Departamento de Ciências Naturais, Universidade Federal de São João del Rei, 36301-160 São João del Rei, MG, Brazil*
[2]*Departamento de Física Teórica, Universidade do Estado do Rio de Janeiro, 20550-013 Rio de Janeiro, RJ, Brazil*
(Received 3 July 2009; revised manuscript received 15 August 2009; published 24 September 2009)

We consider a planar system of fermions, at finite temperature and density under a static magnetic field parallel to the two-dimensional plane. This magnetic field generates a Zeeman effect and then a spin polarization of the system. The critical properties are studied from the Landau's free energy. The possible observable consequences of the magnetization of planar systems such as polymer films and graphene are discussed.

DOI: 10.1103/PhysRevB.80.115428 PACS number(s): 71.30.+h, 36.20.Kd, 11.10.Kk

I. INTRODUCTION

Field theories in two spatial dimensions have long been recognized as important for understanding several physical phenomena that can be well approximated as planar ones, such as high-temperature superconductors and the fractional quantum-Hall effect. In the last years there has been an enormous interest in these two-dimensional systems in condensed-matter physics. In particular, a large number of important new phenomena discovered recently in condensed matter lies in this class. As examples we can cite the metal-insulator transition (MIT) (Ref. 1) and graphene, an isolated single atomic layer of carbon, in which electron transport is essentially governed by Dirac's relativistic equation.[2] It is then feasible to treat many of these planar (or quasiplanar) systems in condensed matter in terms of quantum-field-theory models for fermions in 2+1 dimensions (two space like and one time like coordinates).

Among the many field-theory models useful for understanding a plethora of phenomena in condensed-matter systems, those that include a four-fermion interaction have been extensively used in the context of studies of planar systems. In particular, Nambu-Jona-Lasino type of models[3] in 2+1 dimensions and, among them, the Gross-Neveu (GN) model,[4] have been employed to study these systems. For example, the GN model has been considered as an appropriate model to study low energy excitations of high-temperature superconductors[5] while analogous models with generic quartic fermionic interactions have also been used to study quantum properties of graphene.[6]

In these planar systems, GN field-theory models for fermionic interactions are commonly used to study their symmetry properties, in particular chiral symmetry breaking and restoration, at finite temperature and densities and also in the presence of external (magnetic) fields. In this paper we will be interested in investigating the effects of how an "asymmetrical doping" can affect the chiral symmetry, or the metal-insulator transition in a GN type of model for a two-dimensional system of fermions. An asymmetrical doping can be defined as an imbalance between the chemical potentials of the electrons with the two possible spin orientations ("up" $\equiv\uparrow$ and "down" $\equiv\downarrow$) inserted in the system by a doping process. Since the densities of the $\uparrow$ and $\downarrow$ electrons are directly proportional to their chemical potentials, an asymmetrical doping is equivalent to an asymmetry in the chemical potentials for spin-up and spin-down electrons. This chemical-potential asymmetry can be produced by the effect of an external magnetic field parallel to the system's two-dimensional plane.

A magnetic field applied parallel to the system's two-dimensional plane couples only to the spin of the electrons but not to the electrons orbital motion. Therefore, Landau levels that would appear due to the coupling of a (perpendicular to the plane) magnetic field to the electrons' orbital motion do not appear here. Instead, the in-plane magnetic field generates an intrinsic Zeeman effect which polarizes the system. This is because at zero magnetic field electrons with spin up and spin down have the same density, but an in-plane magnetic field, due to the Zeeman effect, causes a difference between the spin-up and spin-down densities. Recent studies in the context of graphene[7,8] have suggested that the Zeeman effect can be very important for the electronic properties of these systems. The intrinsic Zeeman effect is thus useful to reveal the important role played by the spin degree of freedom of the electron and the polarization of the system.[9]

Here we will focus on the properties of a planar system modeled by a GN four-Fermi interacting model and study how a spin-density asymmetry influences on the chiral symmetry of the system, i.e., on the role of the Zeeman contribution to the system's magnetization. The rest of this paper is organized as follows. In Sec. II, we review the GN model and the effect of including an in-plane constant magnetic field and the Zeeman effect. In Sec. III we evaluate the Landau's free energy (the effective potential) of the model and determine how the chiral symmetry is affected by the spin-density asymmetry. In Sec. IV we determine the magnetic properties of the system. Finally, in Sec. V we present our concluding remarks.

II. THE MODEL ACTION

We start by considering a planar four-Fermi model describing interacting fermions with a Lagrangian density given by

$$\mathcal{L}[\bar{\psi},\psi]=\sum_{s=\uparrow,\downarrow}\bar{\psi}^s(i\hbar\partial_t-i\hbar v_F\vec{\gamma}.\vec{\nabla})\psi^s+\sum_{s=\uparrow,\downarrow}\frac{\lambda}{2N}\hbar v_F(\bar{\psi}^s\psi^s)^2, \tag{1}$$

where ψ^s is a four-fermion field with N flavors and s is an internal symmetry index (spin) that determines the effective

degeneracy of the fermions. In Eq. (1) a sum in the flavors is implicit. For example, for materials such as polyacetylene or graphene, $N=2$. We will keep N general throughout this work for convenience.

In Eq. (1), λ is a coupling term and v_F is the Fermi velocity. The gamma matrices are 4×4 matrices and we follow the representation given, e.g., in Ref. 10 for fermions in 2 +1 dimensions. In this case, the model (1) possesses a discrete chiral symmetry, $\psi\rightarrow\gamma_5\psi$, $\bar{\psi}\rightarrow-\bar{\psi}\gamma_5$, with the γ_5 matrix defined as in Ref. 10. This discrete chiral symmetry is the one considered in this paper, along with its breaking and restoration conditions. Note that it is broken when a gap (or a nonvanishing vacuum expectation value for $\langle\bar{\psi}\psi\rangle$) is generated.

It is useful to rewrite the fermion interaction term in Eq. (1) in terms of a boson field Δ, in which case $\mathcal{L}[\bar{\psi},\psi]$ becomes

$$\mathcal{L}[\bar{\psi},\psi,\Delta]=\sum_{s=\uparrow,\downarrow}\bar{\psi}^s[i\hbar\partial_t-i\hbar v_F\vec{\gamma}.\vec{\nabla}-\Delta]\psi^s-\frac{N}{2\hbar v_F\lambda}\Delta^2. \tag{2}$$

Δ can be seen, for example, as representing the coupling of electrons to a local value of the dimerization. Equation (2) is equivalent to Eq. (1) as can be easily verified by using the field equation for $\Delta(x)$ and substituting it back into the Lagrangian density, reobtaining the characteristic four-Fermi interaction.

Models of the type of Eq. (2), or equivalently Eq. (1), are of the form of a Gross-Neveu model,[4] with applications found in many areas of condensed-matter physics. For example, in one-space dimension, Eq. (2) is the equivalent of the Takayama-Lin-Liu-Maki model,[11] the continuous version of the model proposed by Su, Shrieffer, and Heeger for polyacetylene,[12,13] in the adiabatic approximation, where lattice vibrations are neglected, and used to study the metal-insulator transitions in general (see, e.g., Ref. 14, and references therein).

Let us now consider the application of a generic external magnetic field to the system and its effects. It is convenient that to start by writing the grand canonical partition function for the Lagrangian density model (2),

$$Z=\int D\Delta\prod_s D\psi^\dagger D\psi\exp\{-S_E[\bar{\psi},\psi,\Delta]\}, \tag{3}$$

where the Euclidean action $S_E[\bar{\psi},\psi]$, from the Lagrangian density Eq. (2), reads

$$S_E[\bar{\psi},\psi,\Delta]=\int_0^{\hbar\beta}d\tau\int d^2x\Bigg\{\sum_{s=\uparrow,\downarrow}\bar{\psi}^s\Bigg[\hbar\partial_\tau+i\hbar v_F\gamma_1\times\left(\partial_x+i\frac{e}{c}A_x\right)+i\hbar v_F\gamma_2\left(\partial_y+i\frac{e}{c}A_y\right)+\Delta+\gamma_0\mu+\frac{\sigma_s}{2}\gamma_0 g\mu_B B_\parallel\Bigg]\psi^s+\frac{N}{2\hbar v_F\lambda}\Delta^2\Bigg\}, \tag{4}$$

where $\beta=1/(k_BT)$, k_B is the Boltzmann constant, μ is the chemical potential, A_x and A_y are the vector potential components (e.g., corresponding to a magnetic field perpendicular do the system's plane), $B_\parallel$ is the magnetic field parallel to the system's plane, and $\sigma_s\gamma_0 g\mu_B B_\parallel/2$ is the corresponding Zeeman energy term, with $\sigma_\uparrow=1$, $\sigma_\downarrow=-1$, g is the spectroscopic Lande factor, and μ_B is the Bohr magneton. We must point out that graphene samples have been recently studied in strong magnetic fields (up to 45 T).[15] In these experiments the measured effective g^* factors were found very close to the bare electron g factor ($g=2$). In our work developed below, we will not assign a specific value for g and we keep it also general (like N) for convenience.

By choosing a gauge where the three-dimensional vector potential is given, for example, by $\vec{A}=(0,B_\perp x,B_\parallel y)$, we see from Eq. (4) that $B_\perp$ couples to the orbital motion of the electrons and it will result in the Landau levels for the system in this magnetic field. The parallel magnetic field couples to the electrons' spin and produces the Zeeman energy term in Eq. (4). From the form of the Zeeman energy term in Eq. (4) we see that it can be added to the chemical potential, thus defining an effective chemical-potential term in the action of the form

$$\sum_{s=\uparrow,\downarrow}\mu_s\bar{\psi}^s\gamma_0\psi^s=\sum_{s=\uparrow,\downarrow}\left(\mu+\frac{\sigma_s}{2}g\mu_B B_\parallel\right)\bar{\psi}^s\gamma_0\psi^s=\mu_\uparrow\psi^{\uparrow\dagger}\psi^\uparrow+\mu_\downarrow\psi^{\downarrow\dagger}\psi^\downarrow, \tag{5}$$

where $\mu_\uparrow=\mu+\delta\mu$ and $\mu_\downarrow=\mu-\delta\mu$, with $\delta\mu=g\mu_B B_\parallel/2$. The role of μ can be interpreted as to account for the extra density of electrons that is supplied to the system by the dopants while $\delta\mu$ measures the amount of asymmetry introduced and it is directly proportional to the in-plane applied external magnetic field. As we explained in the introduction, in this work we will be concerned with the effects of the Zeeman term, so from now on we take $B_\perp=0$ and only consider a constant in-plane external magnetic field $B_\parallel\equiv B_0$.

III. THE SYSTEM'S EFFECTIVE POTENTIAL UNDER EXTERNAL EFFECTS

In the applications with models of the GN type, we are mostly interested in studying the effective potential, or Landau's free energy, for a constant scalar field configuration Δ_c, in which case chiral symmetry breaking and dynamical fermion mass generation can be most conveniently studied. Here, we use the effective potential for Δ_c for studying how an asymmetry between the up and down fermions' spins, generated by the constant in-plane magnetic field, will change the phase diagram of the model. Possible phenomenological applications of these results for systems like, for example, graphene and planar organic conductors, as polyacetylene, will then be discussed.

The effective potential is defined from the grand canonical partition function (3) by

$$V_{\text{eff}} = -\frac{1}{\beta \mathcal{V}} \ln Z, \tag{6}$$

where $\mathcal{V}$ is the volume. Then, from the partition function Eq. (3) with Eq. (4) and using Eq. (5), for a constant background scalar field Δ_c and in the mean-field approximation, which is the same as considering just the leading terms in a $1/N$ expansion, or the large-N approximation,[16,17] we obtain that the effective potential V_{eff} is given by

$$V_{\text{eff}}(\Delta_c, T, \mu_\uparrow, \mu_\downarrow) = \frac{N}{2\hbar v_F \lambda}\Delta_c^2 - Nk_B T \sum_{s=\uparrow,\downarrow} \text{tr} \sum_{n=-\infty}^{+\infty} \int \frac{d^2p}{(2\pi\hbar)^2} \ln[(-i\omega_n + \mu_s) - v_F \gamma_0 \vec{\gamma}\cdot\vec{p} - \gamma_0 \Delta_c], \tag{7}$$

where $\omega_n = (2n+1)\pi k_B T$ are the Matsubara frequencies for fermions. Note that in the absence of asymmetrical doping, $\mu_\uparrow = \mu_\downarrow = \mu$, or $\delta\mu = 0$, Eq. (7) just reproduces (in the natural units where $\hbar = k_B = v_F = 1$) the effective potential of the Gross-Neveu model in 2+1 dimensions.[3]

Performing the sum over the Matsubara frequencies and taking the trace in Eq. (7), we find

$$V_{\text{eff}}(\Delta_c, T, \mu_\uparrow, \mu_\downarrow) = \frac{N}{2\hbar v_F \lambda}\Delta_c^2 - 2Nk_B T \int \frac{d^2p}{(2\pi\hbar)^2}\left[\beta E_p + \frac{1}{2}\ln(1 + e^{-\beta E_\uparrow^+}) + \frac{1}{2}\ln(1 + e^{-\beta E_\uparrow^-}) + \frac{1}{2}\ln(1 + e^{-\beta E_\downarrow^+}) + \frac{1}{2}\ln(1 + e^{-\beta E_\downarrow^-})\right], \tag{8}$$

where $E_{\uparrow,\downarrow}^{\pm} = E_p \pm \mu_{\uparrow,\downarrow}$ and $E_p = \sqrt{v_F^2 p^2 + \Delta_c^2}$. In terms of the band structure, we can interpret the result seen in Eq. (8) as like $\delta\mu$ has lifted the degeneracy of the conduction and valence bands in the matter part of V_{eff}.

At zero temperature and chemical potential and in the absence of the external magnetic field, V_{eff} becomes

$$V_{\text{eff}}(\Delta_c) = \frac{N}{2\hbar v_F \lambda}\Delta_c^2 - 2N \int \frac{d^2p}{(2\pi\hbar)^2}\sqrt{v_F^2 p^2 + \Delta_c^2}. \tag{9}$$

By using a momentum cutoff Λ to regulate the vacuum divergent term of $V_{\text{eff}}(\Delta_c)$ and by defining a renormalized coupling λ_R as

$$\frac{1}{\lambda_R} = \frac{\hbar v_F}{N}\frac{d^2 V_{\text{feff}}(\Delta_c)}{d\Delta_c^2}\bigg|_{\Delta_c = \Delta_0}, \tag{10}$$

where Δ_0 is a renormalization point, that can be chosen, as usual, as given by the nontrivial minimum of the renormalized effective potential.

In terms of λ_R, the renormalized effective potential reads (after subtracting an irrelevant field-independent divergent vacuum term)

$$V_{\text{eff},R}(\Delta_c) = \frac{N}{2\hbar v_F \lambda_R}\Delta_c^2 + \frac{N}{\pi(\hbar v_F)^2}\left(\frac{|\Delta_c|^3}{3} - |\Delta_0|\Delta_c^2\right). \tag{11}$$

The nontrivial minimum of $V_{\text{eff},R}(\Delta_c)$ can now be easily found and it is given by

$$\Delta_0 = \frac{\hbar v_F \pi}{\lambda_R}. \tag{12}$$

At $\Delta_c = \Delta_0$, the effective potential reads

$$V_{\text{eff},R}(\Delta_c = \Delta_0) = -\frac{N}{(\hbar v_F)^2}\frac{\Delta_0^3}{6\pi}, \tag{13}$$

which shows that $V_{\text{eff}}(\Delta_c = \Delta_0) < V_{\text{eff}}(\Delta_c = 0) = 0$. The nontrivial solution is then energetically preferable for the (undoped) system, which then corresponds to a (dynamical) gap, i.e., the presence of a chiral nonvanishing vacuum expectation value.

The effective potential at finite chemical potentials and in the zero-temperature limit, from Eq. (8), is given by

$$V_{\text{eff},R}(\Delta_c, \mu_{\uparrow,\downarrow}) = V_{\text{eff},R}(\Delta_c) + N\Theta_1 \int_0^{p_F^\uparrow} \frac{pdp}{2\pi\hbar^2}(E_p - \mu_\uparrow) + N\Theta_2 \int_0^{p_F^\downarrow} \frac{pdp}{2\pi\hbar^2}(E_p - |\mu_\downarrow|), \tag{14}$$

where $V_{\text{eff},R}(\Delta_c)$ is given by Eq. (11), $\Theta_{1,2} = \Theta(\mu_{\uparrow,\downarrow}^2 - \Delta_c^2)$ is a step function, defined as $\Theta(x) = 0$, for $x < 0$, and $\Theta(x) = 1$, for $x > 0$, and $p_F^{\uparrow,\downarrow}$ is the Fermi momentum of the $\uparrow(\downarrow)$ fermions

$$p_F^{\uparrow,\downarrow} = \frac{1}{v_F}\sqrt{\mu_{\uparrow,\downarrow}^2 - \Delta_c^2}. \tag{15}$$

By performing the momentum integration in Eq. (14), we obtain

$$V_{\text{eff},R}(\Delta_c, \mu_{\uparrow,\downarrow}) = V_{\text{eff},R}(\Delta_c) + \frac{N\Theta_1}{4\pi(\hbar v_F)^2}\left(-\frac{\mu_\uparrow^3}{3} - \frac{2}{3}|\Delta_c|^3 + \mu_\uparrow \Delta_c^2\right) + \frac{N\Theta_2}{4\pi(\hbar v_F)^2}\left(-\frac{|\mu_\downarrow|^3}{3} - \frac{2}{3}|\Delta_c|^3 + |\mu_\downarrow|\Delta_c^2\right). \tag{16}$$

Minimizing $V_{\text{eff},R}(\Delta_c, \mu_{\uparrow,\downarrow})$ with respect to Δ_c yields again the trivial solution ($|\Delta_c| = 0$) and

$$|\Delta_c| - \Delta_0 + \frac{\Theta_1}{2}(\mu_\uparrow - |\Delta_c|) + \frac{\Theta_2}{2}(|\mu_\downarrow| - |\Delta_c|) = 0. \tag{17}$$

Before continuing, lets us specialize to the symmetric limit, $\delta\mu = 0$. In this case Eq. (17) reads $|\Delta_c| - \Delta_0 + \Theta(\mu^2 - \Delta_c^2)(\mu - |\Delta_c|) = 0$. To solve this equation we need to know the critical chemical potential μ_c at which the symmetry is restored. This is found through the equation $V_{\text{eff},R}(\Delta_c = 0, \mu_c) = V_{\text{eff},R}(\Delta_c = \Delta_0, \mu_c)$, which yields $\mu_c = \Delta_0$. Thus, the ground state of the symmetric system is characterized by

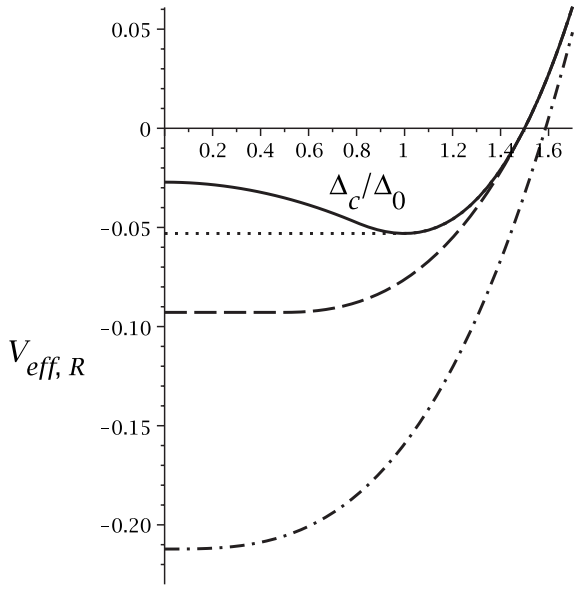

FIG. 1. The effective potential at zero temperature, Eq. (16), in units of $N\Delta_0^3/(\hbar v_F)^2$. The top curve (solid line) is for $\mu=0.8\ \mu_c$ and $\delta\mu/\Delta_0=0$, with the minimum of $V_{\mathrm{eff},R}$ at $\Delta_c=\Delta_0$. The dotted line is for $\mu=\mu_c$, and $\delta\mu/\Delta_0=0$, with the minimum of $V_{\mathrm{eff},R}$ at $\Delta_c=\Delta_0$ and at $\Delta_c=0$. The following curves are for $\delta\mu/\Delta_0=0.5$ (dashed line) and $\delta\mu/\Delta_0=1.0$ (dash-dotted line).

$$\Delta_c=\begin{cases}\Delta_0, & \text{for } \mu<\mu_c\\ 0, & \text{for } \mu\geq\mu_c.\end{cases} \tag{18}$$

At and beyond the doping level μ_c, we note that the energy of the fermions is linear, $E_p=v_F p$, characteristic of two-dimensional gapless systems.[18] Considering now the asymmetrical system case, we see that by applying a constant magnetic field B_0 parallel to the plane, the asymmetry $\delta\mu$ is increased as B_0 increases. We study the asymmetry relative to μ and look at the system's ground state for a given asymmetry. In Fig. 1 we show the effective potential $V_{\mathrm{eff},R}(\Delta,\mu_{\uparrow,\downarrow})$ as a function of Δ_c for various asymmetries $0<\delta\mu/\Delta_0<1$. The first curve in Fig. 1 is the effective potential $V_{\mathrm{eff},R}$ as a function of Δ_c/Δ_0 for $\mu=0.8\mu_c$ and $\delta\mu/\Delta_0=0$ with the minimum of $V_{\mathrm{eff},R}$ at $\Delta_c=\Delta_0$. The second curve from top to bottom shows the symmetry restoration, where $\mu=\mu_c$, and $\delta\mu/\Delta_0=0$. The following curves are for $\delta\mu/\Delta_0=0.5$ and $\delta\mu/\Delta_0=1.0$. These results, in particular, show that there is not a value for an asymmetry $\delta\mu$ for which a new minimum, where $\Delta_c(\delta\mu)\neq 0$, could appear. This is clearly seen from the third and fourth curves in Fig. 1 (from top to bottom), which show that the minimum of the effective potential is always at $\Delta_c=0$. This result should be contrasted with the one obtained for the one-dimensional space system case recently studied,[19] where by increasing the asymmetry, a new minimum for the effective potential emerges at a critical chemical-potential asymmetry $\delta\mu_c$. Thus, a nonvanishing and stable gap beyond $\delta\mu_c$ would exist, till it disappears completely at $\delta\mu\gg\delta\mu_c$, through a second-order phase transition. The absence of this new minimum in our case will be explained below.

Finally, let us now consider the complete renormalized effective potential at both finite chemical potential and temperature, obtained from Eq. (8) after performing the momentum integrals. It is given by

$$\begin{aligned}V_{\mathrm{eff}}(\Delta_c,T,\mu_\uparrow,\mu_\downarrow)=V_{\mathrm{eff},R}(\Delta_c)+\frac{|\Delta_c|}{2\pi\beta^2}\{&\mathrm{Li}_2[-e^{-\beta(\Delta_c-\mu_\uparrow)}]\\&+\mathrm{Li}_2[-e^{-\beta(\Delta_c+\mu_\uparrow)}]\}\\&+\frac{1}{2\pi\beta^3}\{\mathrm{Li}_3[-e^{-\beta(\Delta_c-\mu_\uparrow)}]\\&+\mathrm{Li}_3[-e^{-\beta(\Delta_c+\mu_\uparrow)}]\}+(\mu_\uparrow\to|\mu_\downarrow|),\end{aligned} \tag{19}$$

where $\mathrm{Li}_\nu(z)$ is the polylogarithm function and it is defined (for $\nu>0$) as[20]

$$\mathrm{Li}_\nu(z)=\sum_{k=1}^{\infty}\frac{z^k}{k^\nu}.$$

From Eq. (19) we can now verify how the Zeeman term, manifested by the density asymmetry term $\delta\mu$, changes the usual (for $\delta\ \mu=0$) chiral phase transition in the GN model when both finite chemical potential and temperature are considered. We start by deriving the gap equation

$$\frac{\partial}{\partial\Delta_c}V_{\mathrm{eff}}(\Delta_c,T,\mu_\uparrow,\mu_\downarrow)|_{\Delta_c=\bar{\Delta}_c(T,\mu_\uparrow,\mu_\downarrow)}=0, \tag{20}$$

which gives

$$\begin{aligned}\bar{\Delta}_c=\Delta_0-\frac{1}{2\beta}\{&\ln[1+e^{-\beta(\bar{\Delta}_c+\mu+\delta\mu)}]+\ln[1+e^{-\beta(\bar{\Delta}_c-\mu-\delta\mu)}]\\&+\ln[1+e^{-\beta(\bar{\Delta}_c+|\mu-\delta\mu|)}]+\ln[1+e^{-\beta(\bar{\Delta}_c-|\mu-\delta\mu|)}]\}.\end{aligned} \tag{21}$$

It can be easily checked that the $T=0$ limit of the above equation reproduces the result Eq. (17). The critical curve $\bar{\Delta}_c(T,\mu,\delta\mu)=0$, that is obtained from Eq. (21), in the case $\delta\mu=0$, just reproduces the known result,[10] with a line for a second-order phase transition in the $\mu-T$ plane, starting at the critical point $(\mu=0,\ T=T_c)$, where $k_BT_c=\Delta_0/(2\ln 2)$, and ending in a first-order critical point at $(\mu=\mu_c,\ T=0)$. By increasing the asymmetry (the magnitude of the parallel magnetic field B_0) the effect is to promote chiral symmetry restoration, as can be explicitly seen in Fig. 2.

We can now interpret the nonexistence here of new minima at $\mu=\mu_c$ in the presence of an asymmetry, in contrast to the findings of Ref. 19 for the one-space dimension case. This can be traced to the nonexistence of a critical line for first-order chiral phase transition in the GN model in two-space dimensions in the mean-field approximation. The phase diagram of the GN model in one-space dimension, in the mean-field approximation, has a second-order critical transition line in the $\mu-T$ plane that meets a first-order transition line at a tricritical point. This is actually a typical phase diagram seen in many other four-Fermi interacting models, including Nambu-Jona-Lasino type of models in three space dimensions. However, this typical phase diagram was absent in the two-space dimensions GN model until

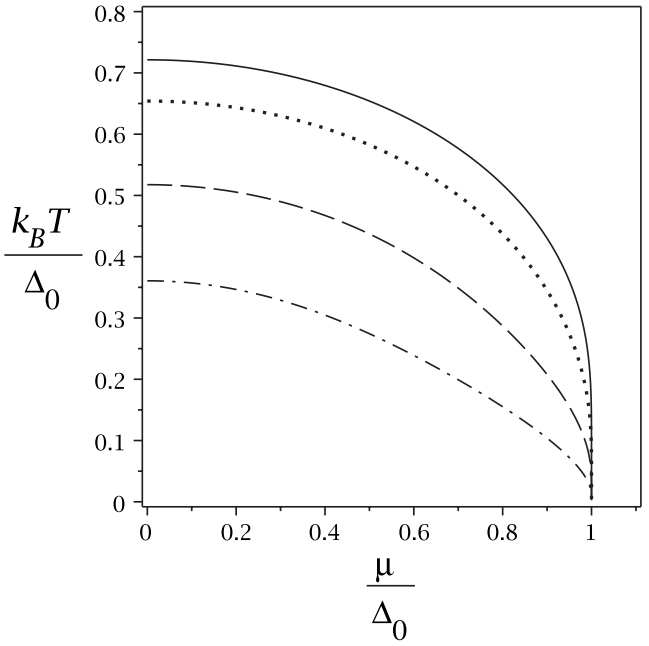

FIG. 2. The critical curve $\bar{\Delta}_c(T,\mu,\delta\mu)=0$ for different values of asymmetry. The top curve (solid line) is for $\delta\mu=0$, while the other curves are for $\delta\mu=0.5\ \mu_c$ (dotted line), $\delta\mu=0.8\ \mu_c$ (dashed line) and $\delta\mu=0.95\ \mu_c$ (dash-dotted line), respectively.

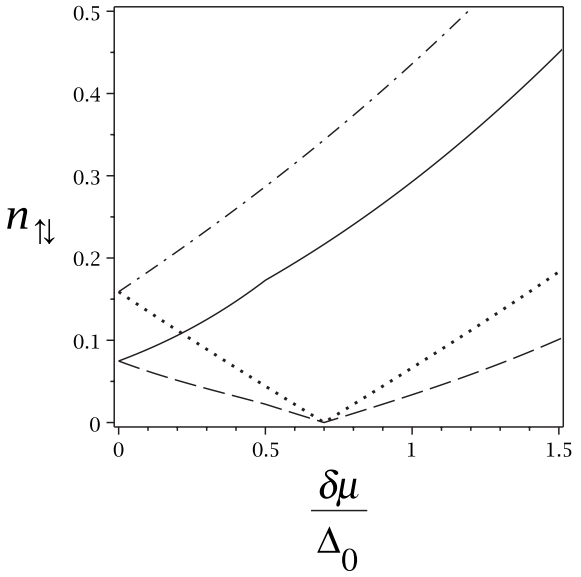

FIG. 3. The number densities of spin-up and spin-down fermions as a function of the asymmetry, for $\mu=0.7\Delta_0$ and for temperatures $k_BT=0.5\Delta_0$ (solid and dashed lines, for $n_\uparrow$ and $n_\downarrow$, respectively) and for $k_BT=\Delta_0$ (dash-dotted and dotted lines, for $n_\uparrow$ and $n_\downarrow$, respectively).

recently.[21] In Ref. 21 it was shown that terms contributing to the effective potential going beyond the mean-field approximation would produce a first-order critical line merging with the second-order critical line at a tricritical point. The effect of the asymmetry close to the critical point μ_c seen in Ref. 19 would then probe the metastable region around the first-order critical line, manifested by the formation of a new local minimum in the presence of an asymmetry. The same should be seen here, if corrections beyond the mean-field approximation would have been considered. We do not see this formation of a new local minimum close to the first-order critical point here because the mean-field approximation in the two-space dimensional GN model misses this metastable region. We expect, though, that these corrections would produce a very small effect here. This is because the metastable region seen in Ref. 21 was considerable smaller than the one in the one-space dimensional GN model so its contributions to our derivations should, likewise, be small.

IV. MAGNETIC PROPERTIES

As we have already seen, the imbalance in the chemical potentials of the $\uparrow$ and $\downarrow$ electrons are induced by the application of a static in-plane magnetic field in the system, with a Zeeman energy $E_Z=\pm g\mu_B B_0/2$ and, in the present case, $\delta\mu=|E_Z|=g\mu_B B_0/2$. As a consequence, the number densities $n_\uparrow$ and $n_\downarrow$, defined by

$$n_{\uparrow,\downarrow}=-\frac{\partial}{\partial\mu_{\uparrow,\downarrow}}V_{\mathrm{eff},R}(\bar{\Delta}_c,\mu_{\uparrow,\downarrow}) \tag{22}$$

are obviously imbalanced due to the asymmetry between $\mu_\uparrow$ and $\mu_\downarrow$, and will depend on $\delta\mu$. Likewise, the spin polarization of the system as a result of the Zeeman effect produces a net (Pauli) magnetization of the system, which is defined by[22]

$$M(T,\mu,\delta\mu)=\frac{g\mu_B}{2}(n_\uparrow-n_\downarrow) \tag{23}$$

and a magnetic (Pauli) susceptibility

$$\chi(T,\mu,\delta\mu)=\frac{\partial}{\partial B_0}M(T,\mu,\delta\mu). \tag{24}$$

Note that the polarization state of the system is determined by the asymmetry which depends on the intensity of the applied magnetic field. As we change the magnetic field, and then the polarization, we expect the magnetic properties of the system, e.g., the magnetization and the susceptibility, to change as well. As we are going to see, the change in behavior can be quite remarkable, mostly when the susceptibility as a function of temperature is concerned.

Let us start by presenting some results for the number densities for fermions of spin up and spin down, as given by Eq. (22). We consider first the case of $\mu=0$ which represents the undoped system, i.e., the insulating state at which $\Delta_c=\Delta_0$. Since $\mu=0$ we have effective chemical potentials given by $\mu_\uparrow=\delta\mu$ and $\mu_\downarrow=-\delta\mu$. From Eq. (22) and the results of the previous section, one sees that if $\delta\mu<\Delta_0$, than $n_\uparrow=n_\downarrow=0$, giving $M=\chi=0$. On the other hand, if $\delta\mu>\Delta_0$, there are nonvanishing densities but they are always equal $(n_\uparrow=n_\downarrow)$ resulting again in $M=\chi=0$. This means that the undoped (insulating) system, for which $\mu=0$, is never magnetized (polarized) at any temperature. So, let us then consider the cases where $\mu\neq 0$. In Fig. 3 we show how the spin-up and spin-down fermion densities [in units of $N\Delta_0^2/(\hbar v_F)^2$] change with the asymmetry (i.e., when the applied magnetic field

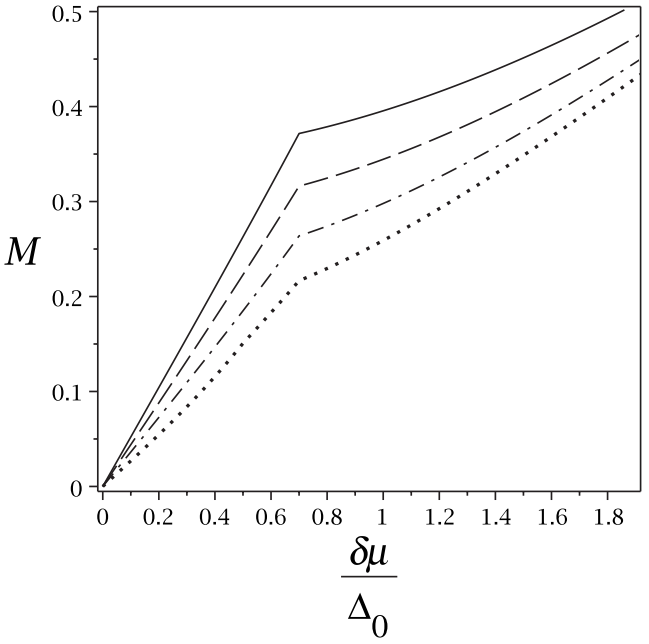

FIG. 4. The Pauli magnetization as a function of the asymmetry, for $\mu=0.7\Delta_0$ and for $k_BT=0.5\Delta_0$ (dotted line), $0.7\Delta_0$ (dash-dotted line), $0.9\Delta_0$ (dashed line) and $1.1\Delta_0$ (solid line).

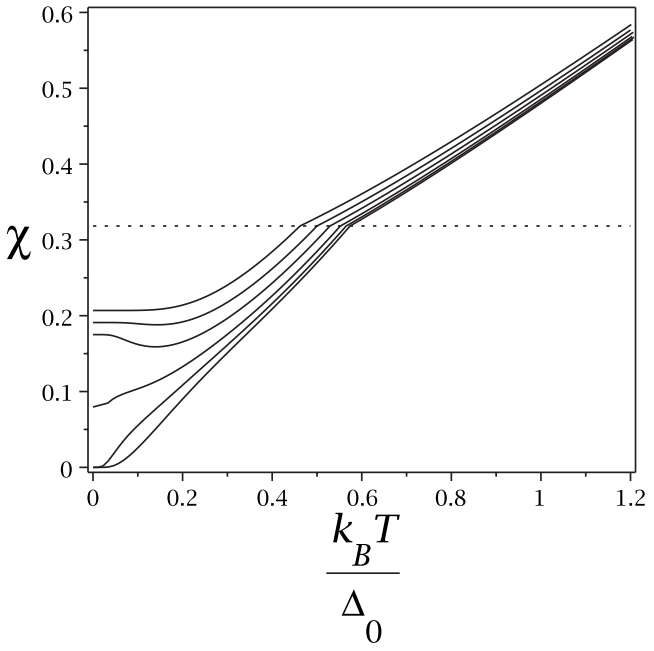

FIG. 5. The Pauli magnetic susceptibility as a function of the temperature for $\mu=0.7\Delta_0$, for the values of the asymmetry $\delta\mu$ (from bottom to top) 0.1, 0.2, 0.3, 0.4, 0.5, and 0.6 (in units of Δ_0). The dotted line indicates where the phase transition happens.

increases), for a chemical potential chosen here, as an example, as $\mu=0.7$, $\mu_c\equiv 0.7\Delta_0$ and for temperatures $k_BT=0.5\Delta_0$ (solid and dashed lines, for $n_\uparrow$ and $n_\downarrow$, respectively) and for $k_BT=\Delta_0$ (dash-dotted and dotted lines, for $n_\uparrow$ and $n_\downarrow$, respectively). Note that in both cases $n_\downarrow$ initially decreases with the increasing magnetic field, vanishing at the full polarization point $\mu=\delta\mu$, as expected, and starts increasing again beyond that point. This is when the magnetic field becomes strong enough to be energetically favorable to spin-down fermions of the filled valence band to be promoted to the conduction band. This occurs only at finite temperature, since at zero temperature $n_\downarrow$ is always zero at and beyond the critical magnetic field B_c (or the full polarization point).[19] Note that the spin-up fermion density always increases with the applied magnetic field (which is in the same direction of the spin-up fermions). The plots also indicate that the rate of spin-down fermions turning into spin-up ones (below the full polarization point) as the result of increasing the applied magnetic field is constant and is approximately the same rate of promotion (above the full polarization point) of spin-down fermions of the valence band to the conduction band. Another result we can notice from Fig. 3 is that the difference in the two densities, i.e., the Pauli magnetization Eq. (23), is always positive with the increasing magnetic field. This is true for any other values of chemical potential and temperature.

Next, in Fig. 4 we present the results for the Pauli magnetization, expressed in units of $N(g\mu_B/2)\Delta_0^2/(\hbar v_F)^2$, for different values of temperature (and again fixing the chemical potential as $\mu=0.7\Delta_0$ for comparison purposes) when the asymmetry is increased (or, equivalently, in terms of the Zeeman field B_0). Here we can easily see a clear change in behavior of the magnetization as the full polarization point is crossed. The most important observation we can notice from the results seen in the Fig. 4, it is that below the full polarization point, here given by $\delta\mu=0.7\mu_c$ (which is the value of μ that we have considered in the analysis), the larger is the temperature, the larger is the rate of increase in the magnetization, while has an opposite behavior above the full polarization point. This then will reflect remarkably in the Pauli magnetic-susceptibility results. As the temperature is increased, the Pauli magnetic susceptibility should as well increase for magnetic fields below of that which gives the full polarization. Above the full polarization magnetic field, the magnetic susceptibility should decrease with the increasing temperature. This is confirmed by the results presented in Figs. 5 and 6, for the cases below the full polarization point and at and above it, respectively.

Figures 5 and 6 show the magnetic susceptibility, expressed in units of $N(g\mu_B/2)^2\Delta_0/(\hbar v_F)^2$, as a function of temperature, when the asymmetry is varied from $\delta\mu=0.1\Delta_0$ up to $1.1\Delta_0$, with fixed chemical potential $\mu=0.7\Delta_0$. For all other values of chemical potential we find similar behavior for $\chi(T,\mu,\delta\mu)$.

Analyzing the behavior of the magnetic susceptibility χ as a function of the temperature, we find that, for those cases below the full polarization point, e.g., Figure 5, in the chiral broken (insulating) phase ($\bar{\Delta}_c\neq 0$), χ is nonlinear for $T<T_c$, where the values of T_c are indicated by the horizontal dotted line in Fig. 5. This horizontal critical line can be determined explicitly and it is given by $N(g\mu_B)^2\Delta_0/[4\pi(\hbar v_F)^2]$. When this critical line is crossed and we go from the broken (insulating) phase to the symmetric (metal) phase, for $T\geq T_c$ (or $\bar{\Delta}_c=0$), the magnetic susceptibility becomes a linear function of the temperature. Note that the magnetic susceptibility, below the full polarization point, is always an increasing func-

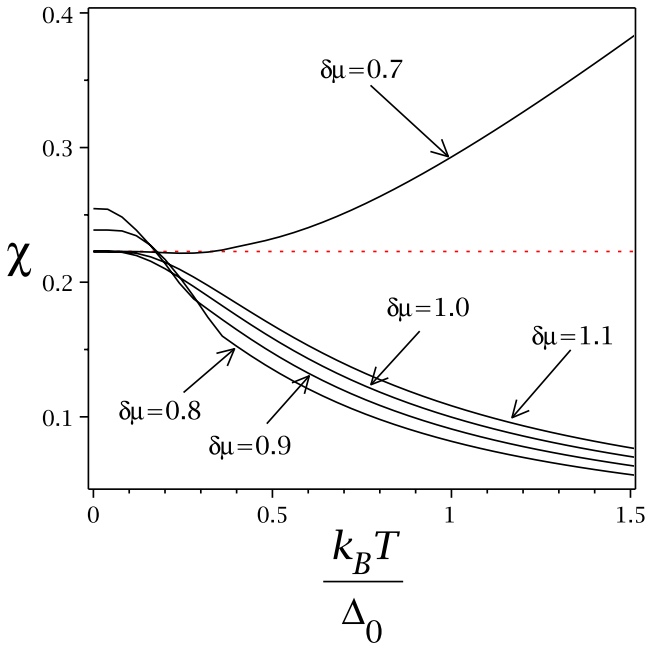

FIG. 6. (Color online) The magnetic susceptibility as a function of the temperature for $\mu=0.7\Delta_0$, for the values of the asymmetry $\delta\mu=0.7,0.8,0.9,1.0,1.1$ (in units of Δ_0).

tion with the temperature, as already anticipated by the behavior of the magnetization seen from Fig. 4.

As we go above the full polarization point, the magnetic susceptibility changes again its behavior with the temperature. We checked that at high temperatures, $k_B T \gg \Delta_0$, it goes exactly as predicted by the Curie-Weiss law,[22] $\chi(\mu < \delta\mu, T \gg \Delta_0) \sim 1/T$. The turning point of behaviors for the magnetic susceptibility, as seen in Figs. 5 and 6, is the full polarization point $\mu=\delta\mu$.

A few analytical results for the magnetic susceptibility can be obtained explicitly. At zero temperature, for any $\mu+\delta\mu<\mu_c$, we find that $\chi(T=0,\mu,\delta\mu)=0$, while for $\mu+\delta\mu \geq \mu_c$, we find that $\chi(T=0,\mu,\delta\mu)\neq 0$. The two curves from bottom to top seen in Fig. 5 correspond to the former case, where $\mu+\delta\mu<\mu_c$. For the cases where $\mu+\delta\mu=\mu_c$, with $\mu<\mu_c$ or $\delta\mu<\mu_c$, which in Fig. 5 corresponds to the third curve from bottom to top, we find the analytical result for the magnetic susceptibility at $T=0$

$$\chi(T=0,\mu+\delta\mu=\mu_c)|_{\mu<\mu_c,\delta\mu<\mu_c}=\frac{N(g\mu_B)^2}{16\pi(\hbar v_F)^2}\Delta_0. \quad (25)$$

At $\mu=\mu_c$, for any $\delta\mu$, or $\mu+\delta\mu\geq\mu_c$ such that $\Delta_c=0$ (see Fig. 1), i.e., in the metal (chiral restored) phase, we find that

$$\chi(T=0,\Delta_c=0)=\frac{N(g\mu_B)^2}{4\pi(\hbar v_F)^2}\Delta_0. \quad (26)$$

This, in particular, corresponds to the values of parameters determining the critical line seen in Fig. 5. The full polarization point can be reached for various dopings and in-plane magnetic fields, i.e., always that $\mu=\delta\mu$, in which case $\mu_\downarrow=0$. In particular, at the full polarization point, for any $\mu>0.5\mu_c$, we find that

$$\chi(T=0,\mu>0.5\mu_c,\mu=\delta\mu)=\frac{N(g\mu_B)^2}{4\pi(\hbar v_F)^2}\mu. \quad (27)$$

We have also verified that this same result for the susceptibility is also obtained for other cases outside the full polarization point, e.g., for $\mu\geq\mu_c$, with any value of the asymmetry $\delta\mu$, or for $\mu>0.5\mu_c$ and $\delta\mu\geq\mu_c$. Note that this result includes the case leading to Eq. (26), for the special case of $\mu=\mu_c$. The curves starting at the dotted line in Fig. 6 correspond exactly to examples of these cases with the dotted line obtained when $\mu=0.7\Delta_0$ is substituted in Eq. (27).

The parameters determining the result given by Eq. (27), together with those determining Eq. (25), show that there are two major regions of parameters, at zero temperature, that preclude the Pauli magnetic susceptibility for attaining a value. We find that the Pauli magnetic susceptibility jumps discontinuously from zero to the value given by Eq. (25), for $\mu+\delta\mu=\mu_c$, with $\mu<\mu_c$ and $\delta\mu<\mu_c$, and then it jumps again from the value given by Eq. (25) to the limiting lower value of susceptibility given by Eq. (27), obtained for $\mu=0.5\mu_c$. For any other possible value that the magnetic susceptibility can have, it will be larger than the value obtained from Eq. (27). This behavior for the magnetic susceptibility could, in principle, be tested experimentally, induced by either a change in chemical potential (e.g., by increasing the doping concentration in planar systems) or by an increase in the magnetic Zeeman field (thus increasing the spin asymmetry).

We also note that, as we have seen in the previous section since for any value of $\mu<\mu_c$ the value of asymmetry $\delta\mu=\mu_c$ will lead to the phase transition. This value of asymmetry corresponds to a critical magnetic field for the chiral phase transition. Since $\delta\mu_c=\Delta_0=g\mu_B B_{0,c}/2$, we find that this critical magnetic field is given by

$$B_{0,c}=\frac{2\Delta_0}{g\mu_B}, \quad (28)$$

where we have used that $\mu_c=\Delta_0$. We may compare this result, for example, with that of MIT (Refs. 1 and 23),

$$B_{\rm pol}=\frac{2E_F}{g^*\mu_B}, \quad (29)$$

where E_F is the Fermi energy, g^* is the effective Lande g factor, and m^* is the effective mass.

V. CONCLUSIONS

To summarize, we have investigated the mean-field phase diagram of planar systems, that can be modeled with a four-Fermi type of model, upon asymmetric doping. We have obtained the magnetization and magnetic susceptibility for this system. The analysis made in this work can be of relevance in studies of many planar systems of interest in condensed matter, like, for example, organic conductors made of polymer films and graphene. In particular, regarding the zero-temperature magnetic susceptibility of these systems, we have predicted that it can change abruptly from zero to the value given by Eq. (25), when increasing either the doping or

the magnetic Zeeman field, such that $\mu_\uparrow$ crosses a critical doping value given by μ_c. Then, it can jump again abruptly up to the point given by Eq. (27) with the minimum value attained for $\mu=0.5\mu_c$. This is a direct prediction of our results that could be tested experimentally.

As far the dependence on temperature is concerned, we have obtained that the magnetic susceptibility can have quite different behaviors depending whether the system is below or above the full polarization point $\mu=\delta\mu$. Below the full polarization point, $\mu<\delta\mu$, while in the chiral broken phase the magnetic susceptibility increases nonlinearly with the temperature, in the chiral symmetric phase it tends to a linear function of the temperature. Unfortunately, it seems that there is still so few or none, to our knowledge, experimental results for the magnetic susceptibility of planar systems of the type that could be modeled by the model studied here, such as planar polymers or graphene, so to be able to compare with our findings. Even so, despite the very different nature, we recall that there are measurements of the behavior of the magnetic susceptibility with the temperature for metal alloys, most notably titanium based,[24] that displays exactly the same behavior as we found here, increasing almost linearly with the temperature, while the sudden change in the susceptibility at the chiral phase-transition point seems to be analogous to the behavior seen in the measured susceptibility of blue bronze ($K_{0.3}MoO_3$) (Ref. 25) and indicative of a Peierls transition there. The behavior of the magnetic susceptibility changes again as we go above the full polarization point. For $\mu<\delta\mu$ the magnetic susceptibility decreases when the temperature increases. In particular, for high temperatures, $T\gg\Delta_0$, it obeys the Curie-Weiss law. The applied magnetic field is then determinant on the type of the behavior observed for the magnetic susceptibility. There is a critical magnetic field, proportional to the chemical potential (the doping concentration) that determines the two behaviors for the magnetic susceptibility as a function of the temperature. We recall that there is a similar behavior seen in pristine graphite,[26] where for low magnetic fields the magnetic susceptibility is observed to increase with the temperature, while for large fields it goes down with the temperature. The major difference there with what we see here is that graphite is diamagnetic while our results reflect the behavior of a paramagnetic material. We hope that in the future there will be measurements of the Pauli magnetic susceptibility for planar systems so to be able to more closely compare with the results we have obtained here.

Our results have also shown that the Zeeman effect in these planar systems tends to weaken the chiral symmetry, thus, the insulating to metal transition may happen at a smaller critical temperature in the presence of a Zeeman field. This behavior, due to an increasing magnetic Zeeman field, is exactly the opposite to what is observed when a perpendicular magnetic field is applied to these systems (see, e.g., Refs. 27 and 28), in which case the chiral symmetry breaking becomes stronger by the effect of the magnetic field and, thus, the transition happens at a higher temperature in the presence of a perpendicular magnetic field. These two opposite effects caused by magnetic fields, when applied parallel or perpendicular to the system's plane, can be a useful tool to regulate the insulating/metal behaviors for these planar systems, when the parallel and perpendicular fields are applied simultaneously and independently, opening interesting possibilities for uses of these type of materials in practical applications as electronic devices. Further studies on the magnetic properties of these systems we hope to make and to report on them elsewhere in the future.

Finally, since in most realistic experiments the measured quantities of interest are related to electric transport, it is expected also in those cases the Zeeman splitting to have important effects. However, a calculation of conductivity effects and transport properties cannot be addressed with the methods we used here, based on the calculation of the effective potential (free energy), which are more suitable for the analysis of the phase structure of the model. But based on experimental studies of an in-plane magnetic field, for example, in graphene, the Zeeman splitting has been shown to be important in both the spin transport and conductance fluctuations properties.[8] It has also been shown that the Zeeman splitting leads to the spectrum of the effective single-particle Hamiltonian exactly as required by the observed pattern of quantization of Hall conductivity.[15] These are interesting effects associated with the electronic transport properties of realistic systems, that we hope to present in the future and based on the model we have studied here.

ACKNOWLEDGMENTS

We thank A. H. Castro Neto and I. Shovkovy for valuable discussions. H.C. and R.O.R. are partially supported by CNPq. H.C. also acknowledges partial support from FAPEMIG.

*hcaldas@ufsj.edu.br
†rudnei@uerj.br

[1] E. Abrahams, S. V. Kravchenko, and M. P. Sarachik, Rev. Mod. Phys. **73**, 251 (2001), and references therein.
[2] K. S. Novoselov, A. K. Geim, S. V. Morozov, D. Jiang, M. I. Katsnelson, I. V. Grigorieva, S. V. Dubonos, and A. A. Firsov, Nature (London) **438**, 197 (2005).
[3] K. G. Klimenko, Z. Phys. C **37**, 457 (1988); B. Rosenstein, B. J. Warr, and S. H. Park, Phys. Rev. D **39**, 3088 (1989); Phys. Rev. Lett. **62**, 1433 (1989).
[4] D. Gross and A. Neveu, Phys. Rev. D **10**, 3235 (1974).
[5] W. Vincent Liu, Nucl. Phys. B **556**, 563 (1999).
[6] J. E. Drut and D. T. Son, Phys. Rev. B **77**, 075115 (2008).
[7] M. Ezawa, J. Phys. Soc. Jpn. **76**, 094701 (2007).
[8] M. B. Lundeberg and J. A. Folk, arXiv:0904.2212 (unpublished).
[9] P. J. H. Denteneer and R. T. Scalettar, Phys. Rev. Lett. **90**, 246401 (2003).
[10] B. Rosenstein, B. Warr, and S. H. Park, Phys. Rep. **205**, 59

(1991).
[11] H. Takayama, Y. R. Lin-Liu, and K. Maki, Phys. Rev. B **21**, 2388 (1980).
[12] W. P. Su, J. R. Schrieffer, and A. J. Heeger, Phys. Rev. Lett. **42**, 1698 (1979); Phys. Rev. B **22**, 2099 (1980).
[13] A. J. Heeger, S. Kivelson, J. R. Schrieffer, and W. P. Su, Rev. Mod. Phys. **60**, 781 (1988).
[14] H. Caldas, J.-L. Kneur, M. B. Pinto, and R. O. Ramos, Phys. Rev. B **77**, 205109 (2008).
[15] Y. Zhang, Z. Jiang, J. P. Small, M. S. Purewal, Y.-W. Tan, M. Fazlollahi, J. D. Chudow, J. A. Jaszczak, H. L. Stormer, and P. Kim, Phys. Rev. Lett. **96**, 136806 (2006); Z. Jiang, Y. Zhang, Y.-W. Tan, H. L. Stormera, and P. Kim, Solid State Commun. **143**, 14 (2007).
[16] S. Coleman, *Aspects of Symmetry* (Cambridge University Press, Cambridge, 1985).
[17] M. Moshe and J. Zinn-Justin, Phys. Rep. **385**, 69 (2003).
[18] A. M. J. Schakel and G. W. Semenoff, Phys. Rev. Lett. **66**, 2653 (1991).
[19] H. Caldas, Nucl. Phys. B **807**, 651 (2009).
[20] *Handbook of Mathematical Functions*, 9th ed., edited by M. Abramowitz and I. A. Steigen (Dover, New York, 1972).
[21] J.-L. Kneur, M. B. Pinto, R. O. Ramos, and E. Staudt, Phys. Rev. D **76**, 045020 (2007).
[22] C. Kittel, *Introduction to Solid State Physics*, 6th ed. (Wiley, New York, 1986).
[23] V. M. Pudalov, G. Brunthaler, A. Prinz, and G. Bauer, Phys. Rev. Lett. **88**, 076401 (2002).
[24] E. W. Collins and P. C. Gehlen, J. Phys. F: Met. Phys. **1**, 908 (1971).
[25] P. Chandra, J. Phys.: Condens. Matter **1**, 3709 (1989).
[26] N.-C. Yeh, K. Sugihara, M. S. Dresselhaus, and G. Dresselhaus, Phys. Rev. B **38**, 12615 (1988).
[27] V. P. Gusynin, V. A. Miransky, and I. A. Shovkovy, Phys. Rev. D **52**, 4718 (1995).
[28] A. S. Vshivtsev, K. G. Klimenko and B. V. Magnitsky, Theor. Math. Phys. **106**, 319 (1996).